Supplement of Atmos. Chem. Phys., 22, 13527–13549, 2022
https://doi.org/10.5194/acp-22-13527-2022-supplement

Atmospheric Chemistry and Physics
Open Access
EGU

Supplement of

An improved representation of aerosol mixing state for air quality–weather interactions

Robin Stevens et al.

Correspondence to: Ashu Dastoor (ashu.dastoor@ec.gc.ca)

1 Detailed description of aerosol partitioning into cloud droplets

In GEM-MACH, the calculation of cloud droplet number concentrations (N_C) depends on whether or not aerosol feedbacks are enabled. In the simulations without aerosol-meteorology feedbacks, aerosol number concentrations have no effect on N_C for the purposes of determining cloud-radiation interactions and all cloud microphysics processes, including rain formation. Instead, N_C for meteorological processes is calculated using a single pre-specified, constant cloud condensation nuclei type and concentration at all points in time and space.

For the purposes of determining aerosol processes, including aqueous chemistry and transport or removal of aerosol within cloud droplets, a diagnostic N_C is calculated based off of the total hydrophilic aerosol number concentration N_A, according to the parameterisation of Jones et al. (1994):

$$N_C = 375(1 - exp(-2.5 \times 10^{-3} N_A)) \tag{1}$$

The N_C calculated in this way may differ from the N_C used for meteorological processes. Here, N_A is calculated by dividing the aerosol volume concentration in the hi-κ mixing-state category in each size bin by the volume of an aerosol particle with the midpoint diameter of the size bin and summing over the size bins. In the SRIM simulation, this reduces to the sum of the total aerosol volume concentration in each size bin divided by the the volume of an aerosol particle with the midpoint diameter of the size bin. The largest N_C particles in the hi-κ mixing-state category are then selected to participate in in-cloud aerosol processes, including aqueous chemistry.

In the simulations with aerosol-meteorology feedbacks enabled, the algorithm described above differs in that N_C is parameterized using Abdul-Razzak and Ghan (2002). Particle hygroscopicity is calculated separately for each mixing-state category based on molecular weights and ion dissociation, as per eq. 7 from Abdul-Razzak and Ghan (2002). Therefore, the aerosol mass in the lo-κ mixing-state categories is included when calculating N_C. The same value of N_C is used both for meteorological processes and aerosol aqueous-phase processes.

However, the largest N_C particles in the hi-κ mixing-state category are still selected to participate in in-cloud aerosol processes, neglecting the aerosol mass in the lo-κ mixing-state category(ies). This may lead to some unphysical behaviour where additional mass in the lo-κ mixing-state category(ies) can lead to smaller aerosol particles in the hi-κ mixing-state category participating in in-cloud aerosol processes, due to the increase in N_C. Investigating this behaviour was beyond the scope of the current work. We intend to improve on the representation of this process in a future version of GEM-MACH, so that the aerosol mass contributing to N_C (in both hi-κ and lo-κ mixing-state categories) is consistent with the aerosol mass participating in in-cloud aerosol processes. This will allow for the possibility of large aerosol particles in lo-κ mixing-state categories to participate in in-cloud aerosol processing and wet deposition.

There are no cloud-borne aerosol tracers transported between chemistry time steps. Instead, aerosol mass is activated as described above. For this portion of the aerosol mass only, aqueous chemistry is calculated, and cloud-to-rain conversion followed by either downwards transport by evaporating precipitation or wet deposition to the surface is accounted for. Afterwards, the new in-cloud aerosol mass is transferred back to the aerosol tracers.

2 Additional Figures

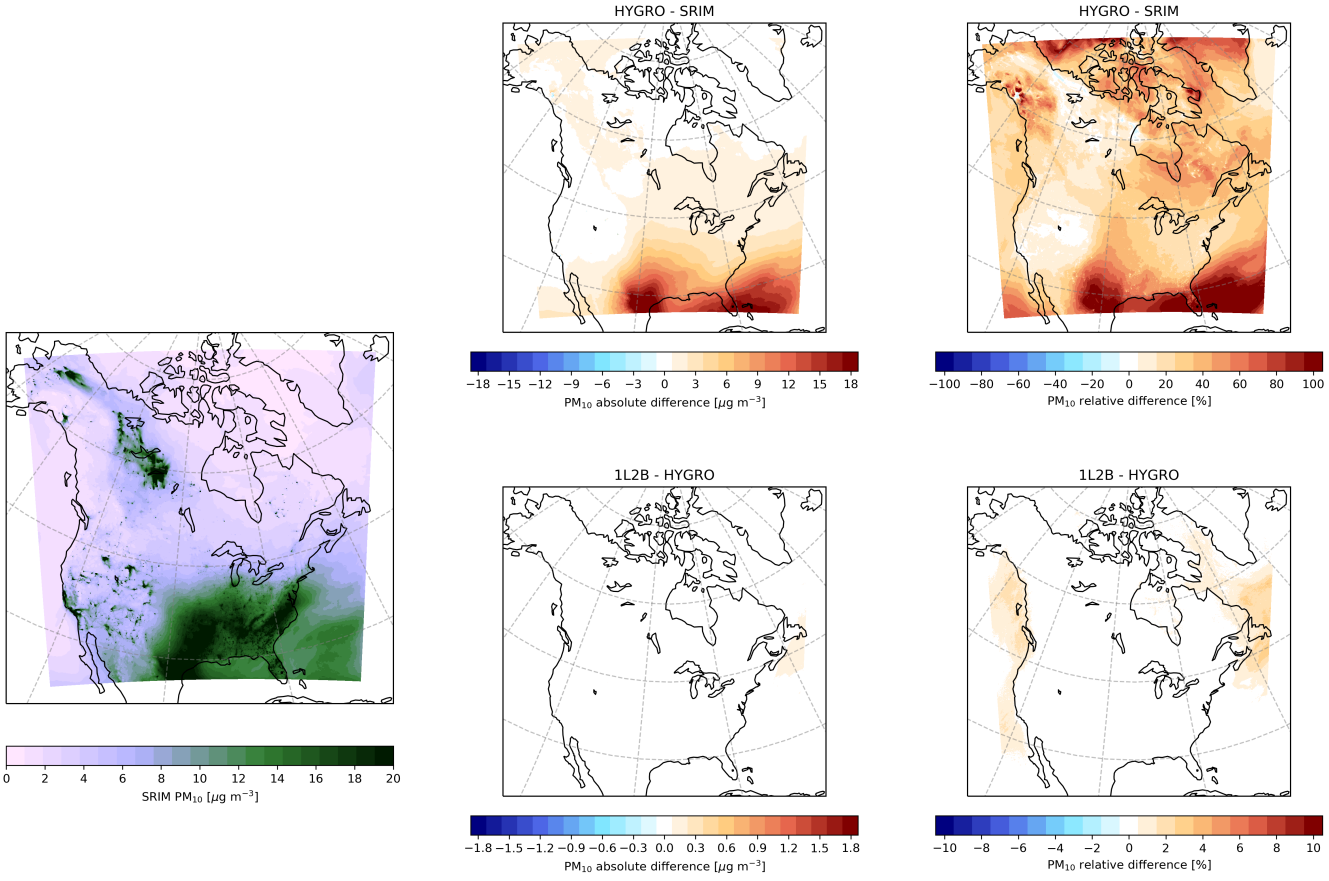

Figure S1. left: mean PM_{10} concentrations from the SRIM simulation; top centre: mean difference in PM_{10} concentrations between the HYGRO and SRIM simulations; top right: relative difference in mean PM_{10} concentrations between the HYGRO and SRIM simulations; bottom centre: mean difference in PM_{10} concentrations between the 1L2B and HYGRO simulations; bottom right: relative difference in mean PM_{10} concentrations between the 1L2B and HYGRO simulations. Note that colour bar scales differ by a factor of ten between subplots in top row and subplots in bottom row.

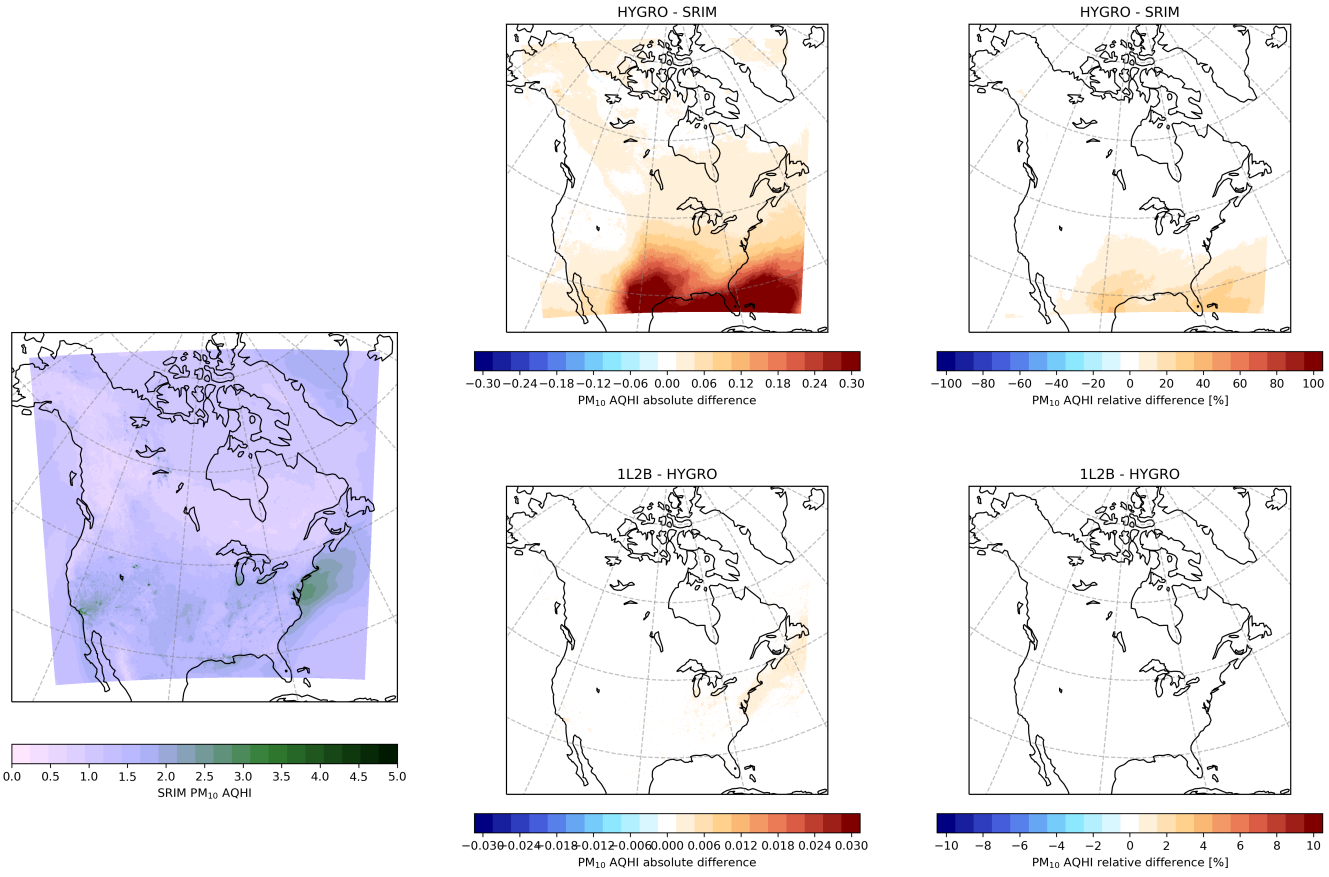

Figure S2. left: mean PM_{10} AQHI values from the SRIM simulation; top centre: mean difference in PM_{10} AQHI values between the HYGRO and SRIM simulations; top right: relative difference in mean PM_{10} AQHI values between the HYGRO and SRIM simulations; bottom centre: mean difference in PM_{10} AQHI values between the 1L2B and HYGRO simulations; bottom right: relative difference in mean PM_{10} AQHI values between the 1L2B and HYGRO simulations. Note that colour bar scales differ by a factor of ten between subplots in top row and subplots in bottom row.

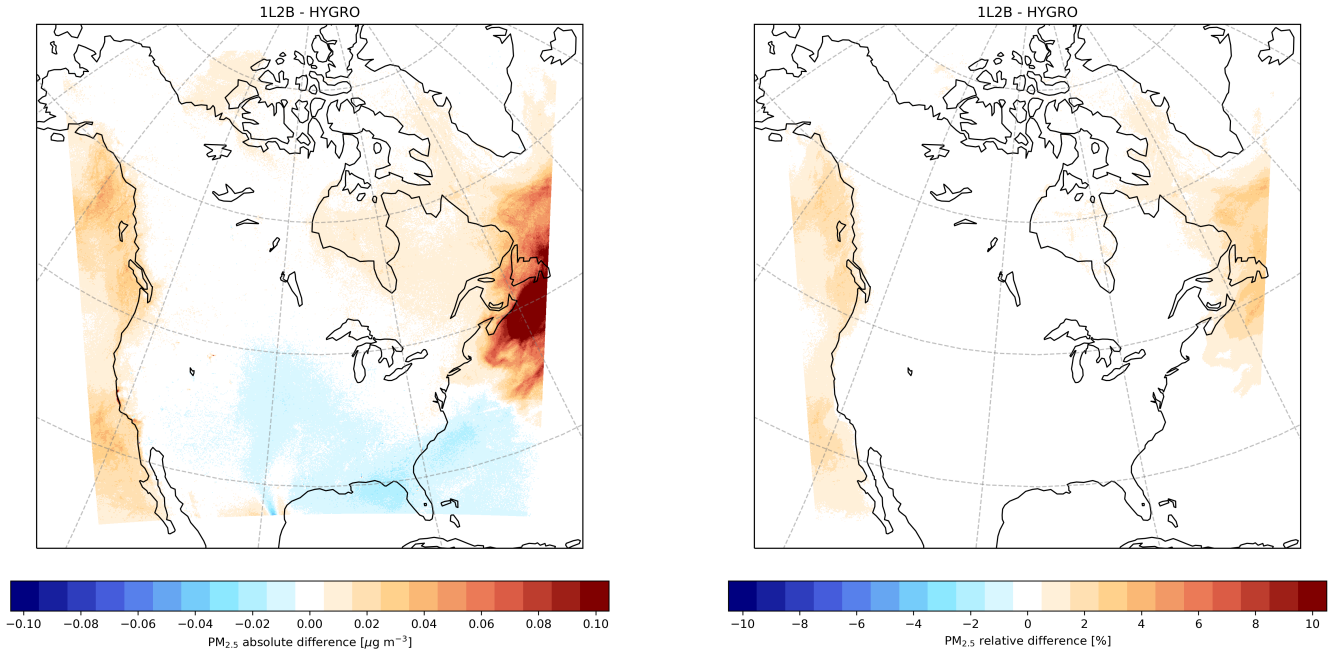

Figure S3. Mean differences in $PM_{2.5}$ values between the 1L2B and HYGRO simulations. left: absolute differences; right: relative differences. Note the finer colour bar scales compared to Fig. 1.

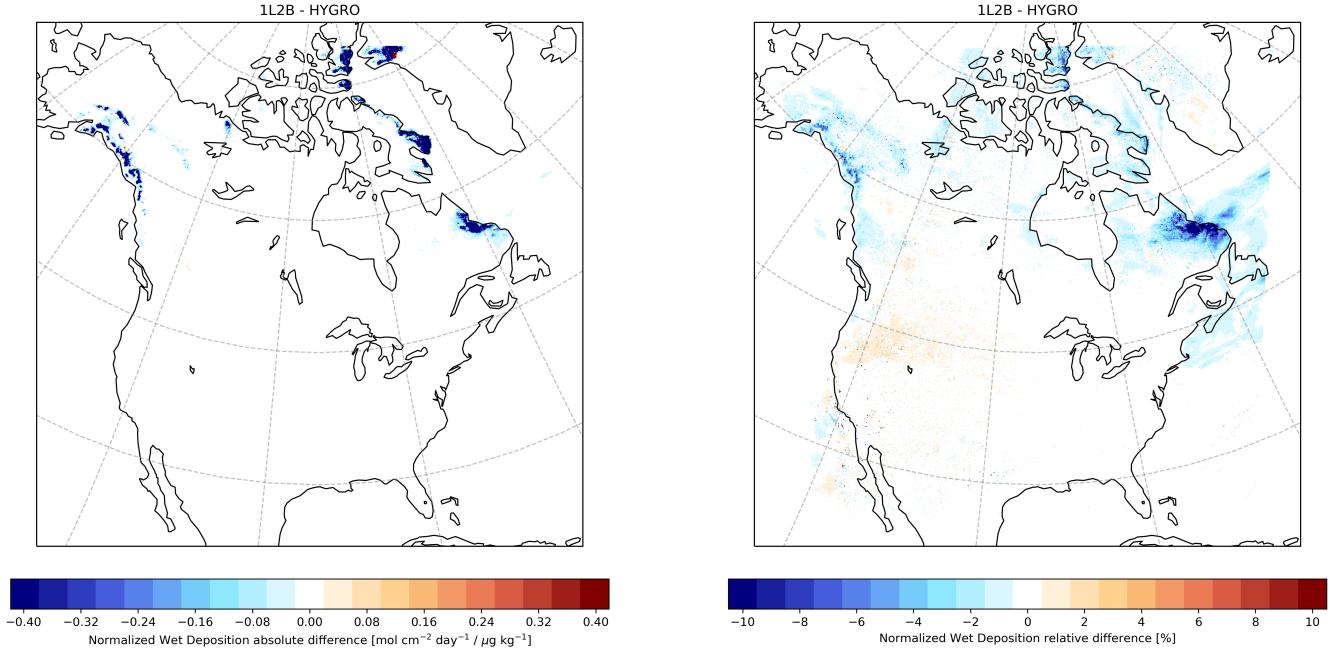

Figure S4. Mean differences in wet deposition fluxes normalized by surface total aerosol concentrations between the 1L2B and HYGRO simulations. left: absolute differences; right: relative differences. Note the finer colour bar scales compared to Fig. 2.

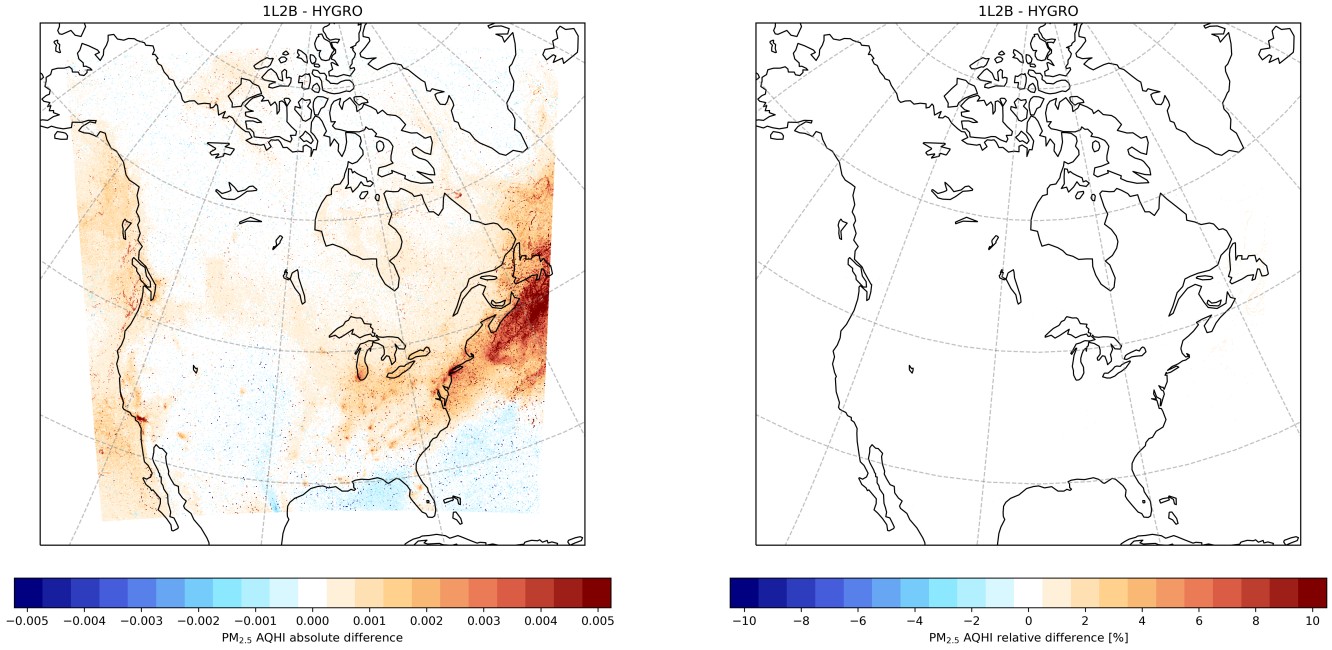

Figure S5. Mean differences in $PM_{2.5}$ AQHI values between the 1L2B and HYGRO simulations. left: absolute differences; right: relative differences. Note the finer colour bar scales compared to Fig. 3.

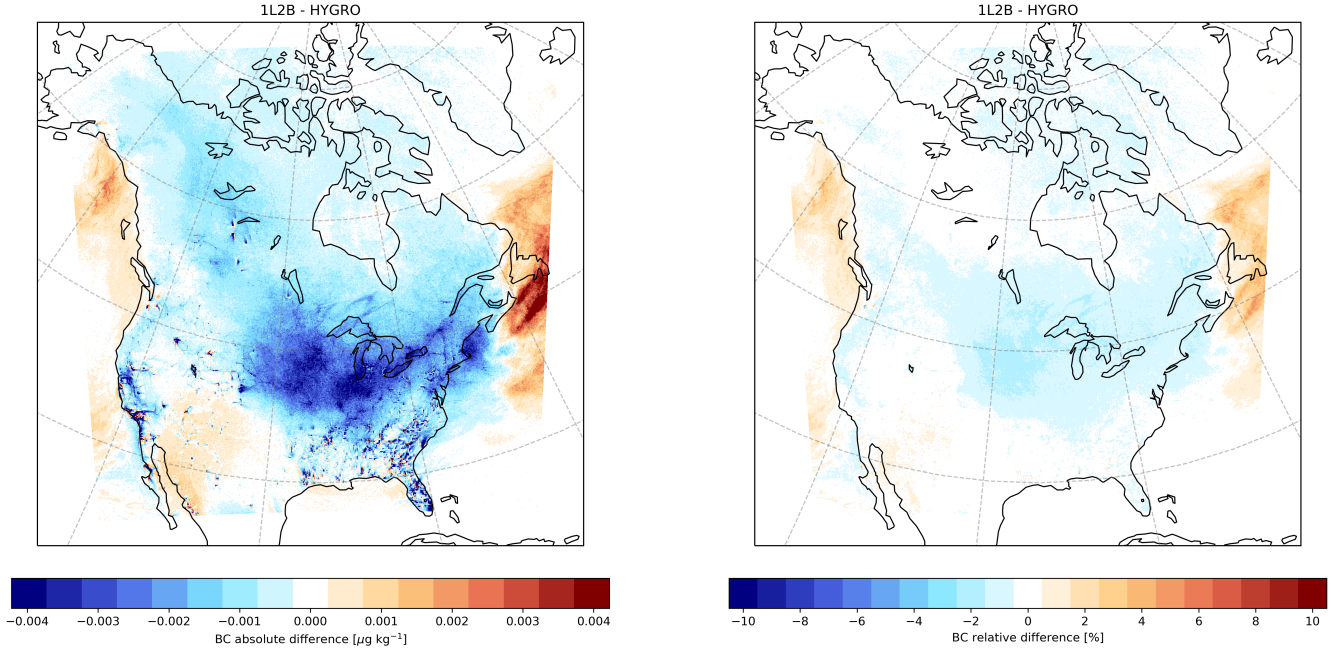

Figure S6. Mean differences in BC surface mixing ratios between the 1L2B and HYGRO simulations. left: absolute differences; right: relative differences. Note the finer colour bar scales compared to Fig. 4.

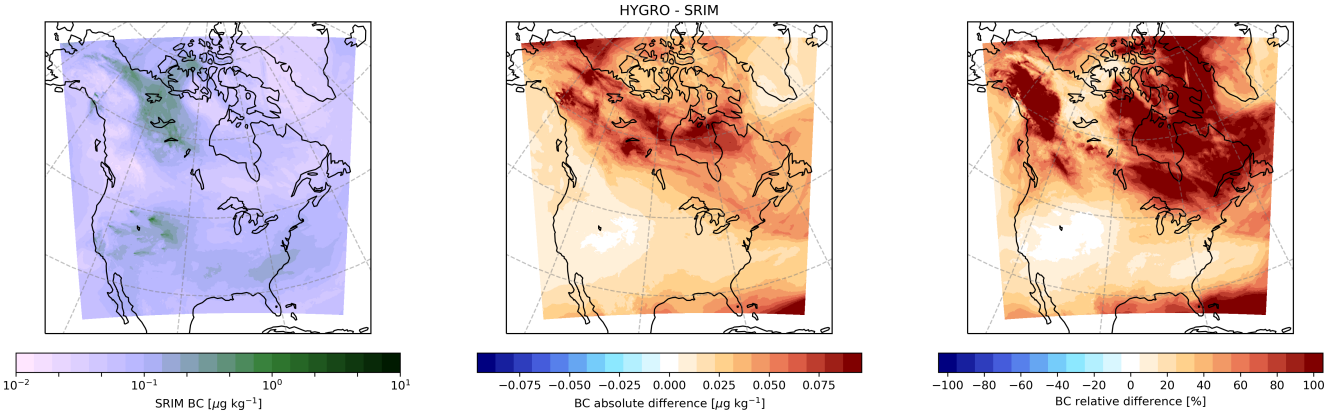

Figure S7. left: mean BC mixing ratios at about 185 hPa above the surface from the SRIM simulation; centre: mean difference in BC mixing ratios between the HYGRO and SRIM simulations; right: relative difference in mean BC mixing ratios between the HYGRO and SRIM simulations.

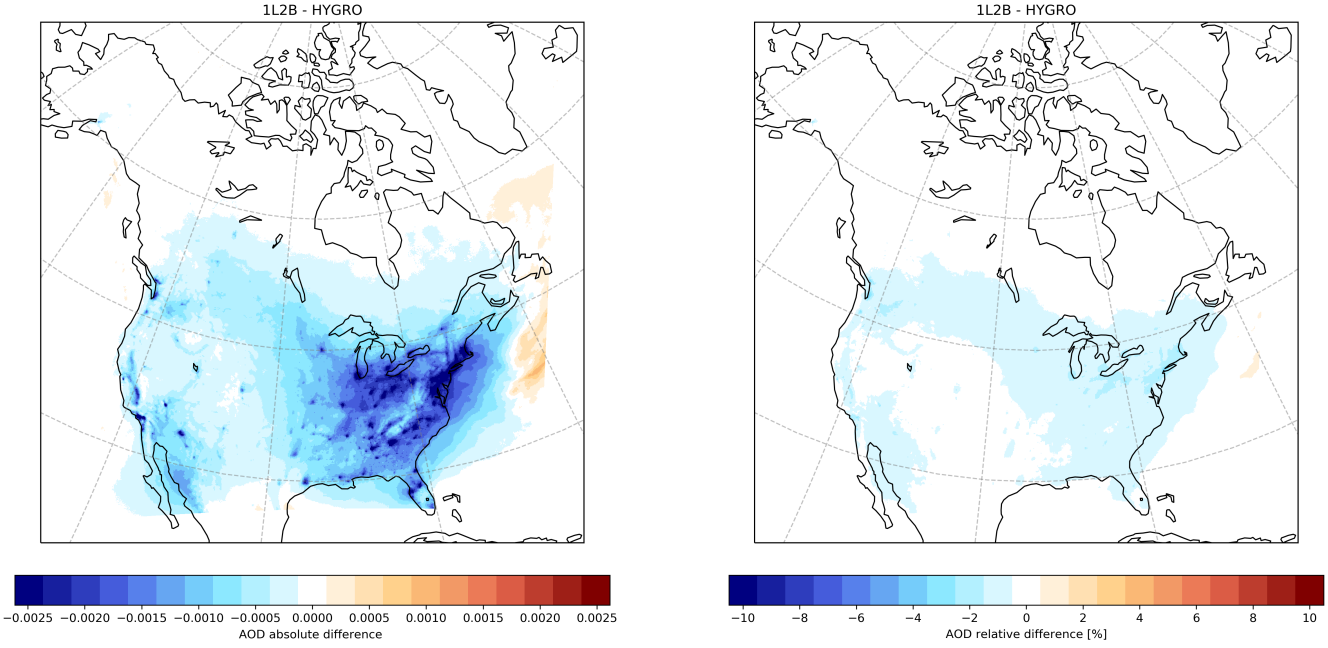

Figure S8. Mean differences in AOD values between the 1L2B and HYGRO simulations. left: absolute differences; right: relative differences. Note the finer colour bar scales compared to Fig. 6.

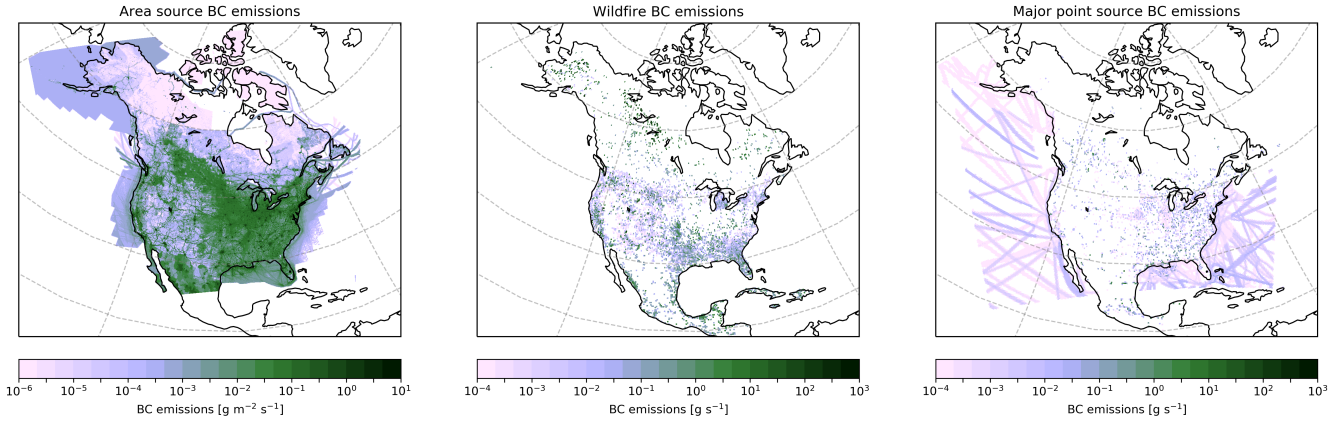

Figure S9. Mean emissions of BC during July 2016. Left: area emissions; centre: emissions from wildfires; right: other major point-source emissions. The wildfire and major point-source emissions are displayed on a 0.25° latitude by 0.25° longitude grid to allow the colours of isolated point sources to be visible. Note the difference in units between area and point sources. Note also that the same source sector (e.g. ocean shipping) can be classified as a major point source in some regions and an area source in others.

References

Abdul-Razzak, H. and Ghan, S. J.: A parameterization of aerosol activation 3. Sectional representation, Journal of Geophysical Research, 107, 4026, https://doi.org/10.1029/2001JD000483, 2002.

Jones, A., Roberts, D. L., and Slingo, A.: A climate model study of indirect radiative forcing by anthropogenic sulphate aerosols, Nature, 370, 450–453, https://doi.org/10.1038/370450a0, 1994.